The analysis of exponential and nonexponential transients in deeplevel transient spectroscopy

P. D. Kirchner, W. J. Schaff, G. N. Maracas, L. F. Eastman, T. I. Chappell, and C. M. Ransom

Citation: Journal of Applied Physics **52**, 6462 (1981); doi: 10.1063/1.328595
View online: http://dx.doi.org/10.1063/1.328595
View Table of Contents: http://scitation.aip.org/content/aip/journal/jap/52/11?ver=pdfcov
Published by the AIP Publishing

The analysis of exponential and nonexponential transients in deep-level transient spectroscopy

P. D. Kirchner, W. J. Schaff, G. N. Maracas, and L. F. Eastman
School of Electrical Engineering, Cornell University, Ithaca, New York 14853

T. I. Chappell and C. M. Ransom
IBM T. J. Watson Research Center, Yorktown Heights, New York 10598

(Received 17 April 1981; accepted for publication 19 June 1981)

One of the major motivations for using computerized waveform capture for deep-level transient spectroscopy is the capability to employ methods of analysis more accurate and informative than boxcars and correlators. Accordingly, we have adapted the fast Fourier transform method and the method of moments to analyze single and multiple exponential decays, respectively. We present relevant details of our experimental system, and compare the boxcar method with the new analyses on both simulated and experimental data. The new analyses have given conclusive, accurate results in cases where the boxcar is ambiguous or directly misleading.

PACS numbers: 06.50.Mk, 71.55.Fr, 72.20.Jv, 78.50.Ge

INTRODUCTION

Deep level transient spectroscopy (DLTS) is a technique well suited to computer automation,[1] but new analyses that make full use of the computer's resources have not been forthcoming. Attempts to analyze deep level transients face the severe signal-to-noise constraints of the experiment and the prevalence of nonideal transients. These nonideal transients consist of nonexponential or multiexponential decays. It is important to note that multiple exponentials are, in fact, nonexponential.

It can be asserted that many experimental data are in fact nonideal on the grounds that the assumptions that led from the thermal emission of carriers by traps to an exponential capacitance transient are somewhat tenuous. The moderate-to-high electric fields of the depletion zone undermine the applicability of the principle of detailed balance,[2] on which the mathematical description of the emission process is based. Large trap concentrations, nonabrupt junctions, and nonuniform doping levels cause nonexponential capacitance transients due to the violation of one or more basic assumptions in the derivation of the capacitance from trap occupation. Even if the deep levels were to yield exponential responses, different levels close in energy would yield an inherently nonexponential sum of exponentials. This can be seen in Fig. 1, which shows a typical optical DLTS transient appearing to contain at least three exponential components.

It has been observed that the conventional methods of anaylsis cannot adequately interpret nonideal transients.[3] Should ideal behavior prevail, however, there is still a need for techniques that better utilize the available data in order to enhance the sensitivity, selectivity, and speed of the experiment.

There are two observations relevant to the analysis of deep level transients. First, a persistent problem is the constant offset of the capacitance or current waveform due to ac coupling of the transient, or simply the equilibrium capacitance or current of the sample when dc coupling is employed. The boxcar and correlator methods are self-restoring: constant offsets subtract themselves out. Other more sophisticated weighting methods[4] also perform restoration. When searching for alternative analysis methods, it should prove useful to look for functions that are similarly insensitive to offset. Second, regardless of the technique employed, it must be reasonable in its computational demands. A typical automated scan of one device records about 400 transients. If the analysis of each transient requires an hour, it is not practical to use this method for DLTS.

FOURIER TRANSFORMS

The Fourier transform has properties that make it exceptionally useful for the analysis of exponential transients. The transform maps a function of time into a function of frequency according to the integral

$$F(\omega)=\int_0^\infty f(t)e^{-i\omega t}dt.$$

Constant offsets appear solely when ω equals zero. For an exponential

$$Ae^{-at}+b$$

and any nonzero angular frequency ω, the ratio of the real

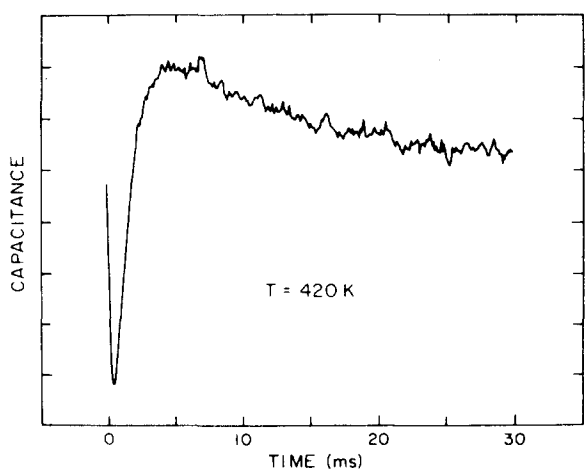

FIG. 1. Optically induced capacitance transient. The data appear to indicate at least three exponential components.

and the imaginary components of $F(\omega)$ yields the quantity $-\alpha/\omega$ independently of the exponential's baseline offset b or amplitude A. The determination of α allows the offset and amplitude to be routinely extracted.

The fast Fourier transform (FFT) implements the Fourier transform in a highly efficient manner. For the FFT, the discrete samples and the finite period t_m are accommodated by the quantization of ω. Because $e^{-i\omega t_m}$ equals one, the ratio of real to imaginary terms of the FFT continues to yield $-\alpha/\omega$ exactly. Therefore, for an N-point FFT, we use the following equations to find α, A, and b.

$$\omega = 2\pi n/t_m \quad \text{for } n = 1,2,\ldots,N-1,$$

$$\alpha = -\omega \mathrm{Re}[\mathrm{FFT}(\omega)]/\mathrm{Im}[\mathrm{FFT}(\omega)],$$

$$A = \frac{\alpha^2+\omega^2}{\alpha}\,\frac{\mathrm{Re}[\mathrm{FFT}(\omega)]\Delta t}{1-e^{-\alpha t_m}} \quad \text{for } \Delta t = \frac{t_m}{N},$$

$$b = \frac{\mathrm{FFT}(0)}{N} - \frac{A(1-e^{-\alpha t_m})}{\alpha t_m}.$$

One must exercise caution that the frequency components introduced by the discontinuity from $f(0)$ to $f(t_m)$ are small with respect to those from the exponential. Typically this can be accomplished by making the first sample equal to the average of the first and the last samples.

One very important feature of this method is that it is noniterative, and hence, despite its accuracy, it is very fast. A fit to a 256-point transient requires about 2.5 sec of microcomputer time. The method gives good results for very noisy signals; in low noise it can extract time constants far in excess of the observed period.

Tests of the FFT method through many fits to both synthesized and experimental data showed its remarkable ability to fit single exponentials accurately. It became increasingly clear, however, that experimental transients did not necessarily consist of single exponentials, and that an analysis that accomodated sums of exponentials was needed to satisfactorily interpret most experimental data.

THE METHOD OF MOMENTS

Serious problems arise in the analysis of multiexponential transients recorded with a finite number of samples and even vanishingly small amounts of noise. A sum of exponentials is essentially degenerate in that, over finite sampling ranges, several sums exist that can fit the available data within experimental error. The terms in each sum can be substantially different from the terms of the of the other sums, yet any two sums cannot simultaneously have physical significance. Each increment of noise increases the set of solutions and compounds the problem of finding a solution with physical validity. The added variable of baseline offset in DLTS data makes the analysis more difficult.

DLTS in not the first experiment to confront the problems posed by multiple exponentials. A group of biochemists[5–7] addressed this problem in the analysis of fluorescence decays of proteins. Their application was similar in that it dealt with sums of exponentials in levels of noise comparable to those common in DLTS. There are, however, several important differences. First, their experiment was based on the recording of one transient. They could afford to make the analysis of each transient highly interactive; we cannot. Second, the observed response times were so short that the excitation pulse was convolved with the response. This is not necessarily the case in DLTS, but the ability to deconvolve the excitation from the response could prove exceptionally useful, especially in optical DLTS. Third, they had no baseline offset. This is the critical factor in the application of the method to DLTS.

The technique they applied was the method of moments, for the exponential components were computed from the time-weighted integrals of the measured response. Our implementation and adaptations of their method follow.

The response function $f(t)$ is taken to consist of a sum of n exponentials. Thus

$$f(t) = \sum_{i=1}^{n} A_i e^{-\alpha_i t},$$

where t is time and A (amplitude) and α (emission rate) pertain to the individual components. If the response is intertwined with an arbitrary excitation waveform $H(t)$, then the method defines a new $F(t)$ as the convolution of $f(t)$ and $H(t)$. In the absence of an excitation pulse, or if $H(t)$ does not interfere with the measurement of $f(t)$, $H(t)$ can arbitrarily be assumed to be a Dirac delta at $t = 0$, in which case

$$F(t) = f(t)$$

both A_i and α_i are unknown. These equations are obtained by taking the time-weighted moments of $F(t)$ and $H(t)$ for integral values of k from zero to $2n$-1.

$$\mu_k = \int_0^\infty t^k F(t)\,dt,$$

$$v_k = \int_0^\infty t^k H(t)\,dt.$$

We can define for a sum of exponentials a quantity G_s

$$G_s = \sum_{i=1}^{n} A_i \tau_i^s \quad \text{for } \tau_i = 1/\alpha_i,$$

and find that we have $2n$ equations

$$\mu_k = k! \sum_{s=1}^{k+1} \frac{G_s v_{k+1-s}}{(k+1-s)!}.$$

If we measure the waveform during the excitation pulse, we measure the excitation waveform and compute both μ_k and v_k using Simpson's rule integration. If the excitation ceases abruptly, we can start the measurements on its falling edge and compute v_k algebraically. These moments are used to calculate the values of G_s. We solve for τ_i from the determinant

$$\begin{vmatrix} 1 & \tau & \tau^2 & \cdots & \tau^n \\ G_1 & G_2 & & & G_{n+1} \\ G_2 & & & & \\ G_n & G_{n+1} & \cdots & G_{2n-1} & G_{2n} \end{vmatrix} = 0$$

by using Gaussian elimination and multiplying the diagonal elements of the matrix to resolve the polynomial in τ, and using algebraic methods to find the roots. These τ_i are the time constants of the components of $f(t)$. Once the values for τ are known, then the amplitudes can be found by using the

calculated values for G_s.

Determination of the moments of $F(t)$ by integration to some finite time introduces potentially substantial truncation error. Therefore, we use the computed values of A_i and τ_i to estimate this error, and iterate until one of three criteria is satisfied: (1) the number of iterations exceeds some maximum, (2) the result is consistent with itself, in that successive iterations do not significantly change the result, (3) the result is consistent with the input. In this third case, the result is as correct as possible.

A technique called exponential depression ensures rapid convergence.[6] The response waveform is multiplied by an arbitrary but well-chosen decaying exponential $e^{-\alpha_d t}$. The extracted amplitudes are unchanged, and the emission rates α_i are related to the extracted τ_i through the simple relation

$$\alpha_i = (1/\tau_i) - \alpha_d.$$

The depressing exponential has beneficial effects because it counteracts problems introduced by truncation error, noise, and baseline offset. The extreme truncation error for gradual decays causes the solution to be quite unstable. The depressing exponential, by increasing the decay rate, results in faster convergence: often the depression will be necessary to achieve convergence at all. The tail of the decay, where the signal-to-noise is at its worst, is also where the function weighted by powers of time is most sensitive. The depressing exponential suppresses this effect. Similarly, if there is a baseline error, $F(t)t^k$ will not converge to zero as t approaches infinity, but $F(t)e^{-\alpha_d t}t^k$ will. This is highly relevant to our application, for the depressing exponential gives the baseline term an emission rate of α_d. This should allow for a routine solution for the baseline as one of the exponential components. Despite its mathematical straightforwardness, the solution poses numerical difficulties most likely introduced by noise and truncation error, and solution for the baseline must be accomplished by forcing a solution for the depressing exponential by synthetic division of the polynomial in τ. Arbitrary convergence does not guarantee the correct answer, and typically one must iterate to successively lighter depressions to obtain a satisfactory solution. This keeps the method under tight control, and usually results in a better solution in less time than if a single, light depression were used.

When implemented in this manner, the method of moments accomplishes one and two component fits at three successively milder depressions (six fits in total) in about 10 sec. Determination of a third component doubles the total time. As a test of the closeness of fit, the program calculates the mean-square error, simply the average of the square of the difference between the input and the fit at each point. This number enables the operator to ascertain the validity of each fit. For compatibility, the other fitting programs generate this number as well.

An interesting approach to the problem of baseline determination for the method of moments is to hybridize the method with the fast Fourier transform. The tail of the decay can usually be approximated by a single exponential, in which case the FFT method can extract the baseline quite accurately. The results are comparable to those obtained using synthetic division. Since the FFT determines the baseline noniteratively, the main advantage of the hybrid approach is speed.

Although we have not yet implemented data smoothing, we feel that we should address the topic because of its potential usefulness. The smoothing should be accomplished by an algorithm that does not introduce nonexponential terms into what is assumed to be a sum of exponentials. The mean displaced ratio,[7] related to autocorrelation, is such a function. It is described numerically as

$$Y_l = \frac{1}{N-L+1}\sum_{i=0}^{N-L}\frac{y_{i+l}}{y_i} \quad \text{for } l = 0,1,\ldots,L \text{ and } L<N,$$

for $N+1$ equally spaced observations y_i. Y vs t has the same time constants of y vs t and amplitudes β_j that are related to the original A_j by

$$\beta_j = \frac{A_j}{N-L+1}\sum_{i=0}^{N-L}\frac{e^{-\alpha_j t_i}}{y_i}.$$

The resulting Y has considerably less noise than y, which more than compensates for the decrease in available samples (L is optimally $\cong 0.9N$).[7] Most importantly, the sum of the β_j is identically one. As with the Fourier transform, one unknown has been removed, and a more accurate fit may result. If y has a substantial baseline offset, however, the offset will predominate in the ratio and suppress the actual transient information. Thus, an accurate approximation of the baseline must be obtained before the mean displaced ratio is employed. Limitations in the method include its requirements that the excitation not coincide with the decay, that measurements be made at equal intervals, and that none of the first $1+N-L$ samples is zero, or is near enough zero to present computational difficulties.

MEASUREMENT

The measurement system shown in Fig. 2 is configured to measure, control, and record the parameters relevant to DLTS. An electrical pulse generator or a Nd:YAG laser and chopper provide the excitation to generate transients. The capacitance signal from a slightly modified Boonton 72B capacitance meter is amplified by a variable gain, low rolloff, ac coupled amplifier before being fed to the analog-to-digital converter. The converter provides 12-bit resolution and programmable gain at rates up to 30 kHz. A programmable clock synchronizes the analog converter by sensing the pulse generator or optical chopper through Schmitt triggers. The computer calculates temperature from the measured thermocouple voltage, and controls temperature through a programmable power supply that feeds resistive heaters on the variable temperature stage. We have found that when a choice exists between implementing a function in software or hardware, usually the software implementation proves much more versatile and reliable. If a feature must be implemented in hardware, it is desirable that it be capable of interfacing with the computer.

The computer, a Digital LSI-11/2, has 28 000 16-bit words of memory. Although it can run at the maximum speed of the analog converter, it can most efficiently convert and accumulate at 100-μs intervals, which, conveniently,

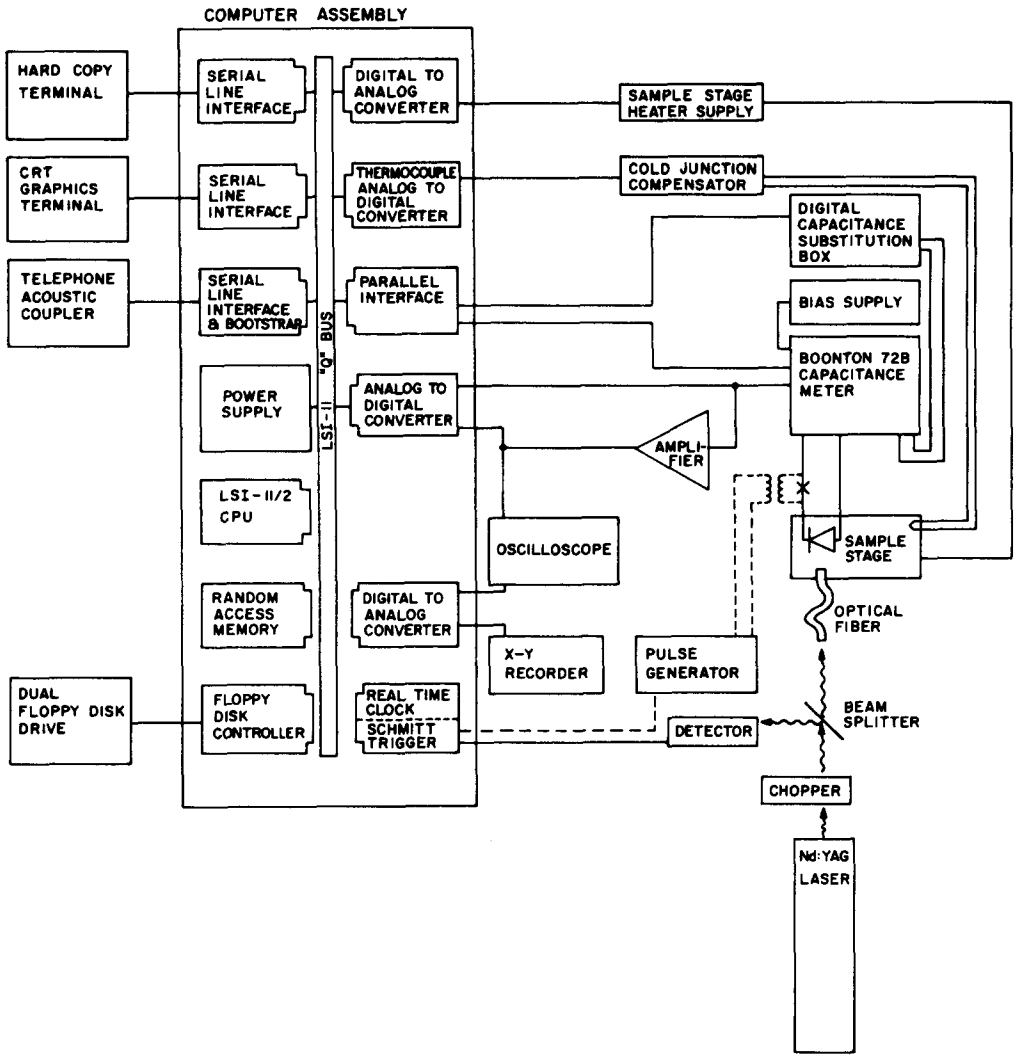

FIG. 2. Configuration of the automated deep level transient spectrometer at Cornell University.

corresponds to the response time of the capacitance meter. To operate at these speeds, certain parts of the measurement program must be implemented in assembly language. The major portions of the program are implemented in FORTRAN, which is compiler-based and hence much faster than an interpreter-based language such as BASIC. Each of two floppy disk drives can store one-half megabyte on removable disks. The typical experiment will scan from 77 to 450 °K, and record sequentially averaged transients to the disk every degree. Usually, the excitation pulses occur at 25 Hz, 300 points are sampled along the decay (30 ms at 100 μs per conversion), and 200 averages occur per degree. Thus the average measurement cycle takes just less than an hour.

Each disk can store the data from two typical runs: exceptionally long data files can be accommodated. The data files are kept for future reference, for the cost of the disks is trivial compared to the cost of the sample and the time involved in its characterization. These archives form a detailed record of experimental experience, enabling studies involving samples than no longer exist. The collection allows rigorous evaluation of data analysis programs. Data that confound current theories and analyses can await future developments.

A unique component of the system, a digitally controlled capacitance substitution box, operates the capacitance meter in the differential mode on a more sensitive scale, with substantial signal-to-noise improvement. This technique for providing a differential capacitance is a distinct improvement over attempts involving varactor diodes. In experimental situations, varactor diodes can cause substantial distortion of the transient due to the flow of current through the sample diode, coupling into the varactor through the capacitance meter. With this adaptation, our detection limit can be as low as one millionth of the net shallow level concentration.

The same computer performs the analyses by reading stored data from the disks. The boxcar, FFT, and moment fitting routines create output files that serve as the input for a general-purpose program that the operator uses to quickly sort through the fit information. The program facilitates tabular printing as well as terminal graphing and X-Y recorder plotting of the data, and permits windowing in order to obtain accurate activation energies and capture cross sections. With a particular trap of interest, the entire cycle from measurement to activation energy determination can be compressed to under 1 h. More exhaustive studies of more levels

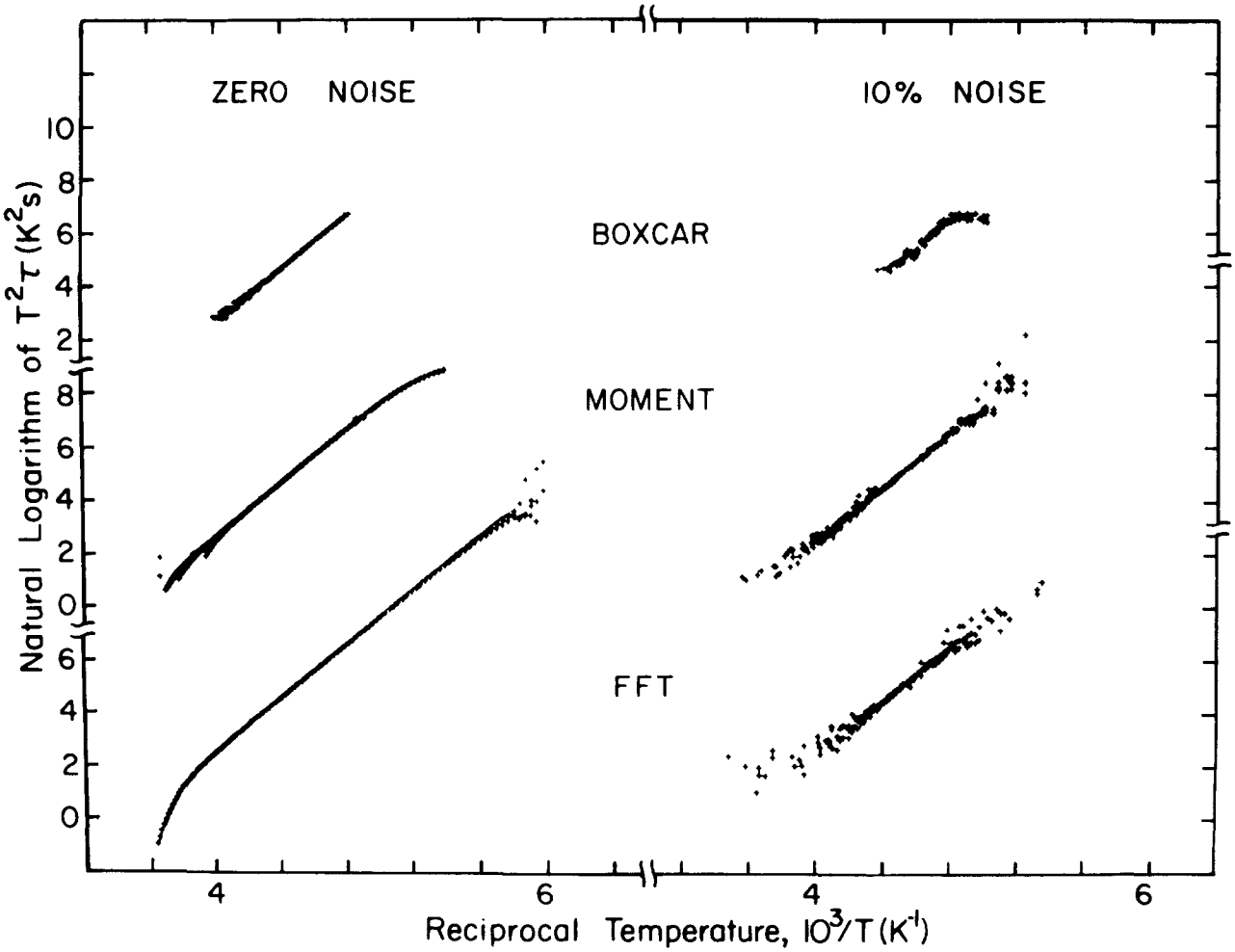

FIG. 3. Boxcar-, moment-, and FFT-derived activation energy plots for a single exponential with 0 and 10% noise.

require, of course, more time. Little human effort is expended, however, for much of this time the computer runs unassisted.

COMPARISONS

We will compare the boxcar, FFT, and moment methods in two stages. In the first step we test the analyses against simulated transients of one and two exponential components with and without noise, and compare the ranges over which the methods provide acceptable answers. In the second step we confront the analyses with experimental data, and make similar comparisons. We chose the boxcar technique for comparison with the new methods because it is by far the predominant procedure for the analysis of DLTS data. Other common methods yield similar results, despite differences in their implementation.[8]

Our system emulates the boxcar in two ways. One program generates boxcar plots from the capacitance C in the conventional $C(t_1) - C(t_2)$ vs T manner, quickly providing a concise summary of the run. The program incorporates expandable gate width for signal-to-noise improvement,[8] and performs peak finding, but does not yet automate activation energy calculations. The second boxcar emulator, employed in the comparison, uses a fixed ratio of t_1 to t_2 and searches for a maximum in magnitude of $C(t_1) - C(t_2)$ *for a single transient at a fixed temperature*. At this maximum, it calculates the decay constant from the well-known formula[8]

$$\tau = (t_1 - t_2)/(\ln t_1 - \ln t_2).$$

Subsequently, it determines the amplitude from

$$A = [C(t_1) - C(t_2)]/[e^{-t_1/\tau} - e^{-t_2/\tau}].$$

The program uses variable gate width for its signal-to-noise benefits, and requires about 1 s to analyze each transient.

This boxcar emulator, by generating its fits of each degree separately, is free of the errors ordinarily caused by transients that change amplitude with temperature. Varying transient amplitude due to changing optical cross section and lack of saturation is recognized as a serious problem in optical DLTS[9] because it can cause substantial errors in the conventional boxcar interpretation. It is essentially impossible to implement this improved boxcar in a hardware system.

A separate program records the simulated transients in a format identical to the measurement program's format, so that the same routines can utilize both sets of data. From the activation energy ΔE and the apparent cross section σ, the time constant τ of the trap at temperature T is determined

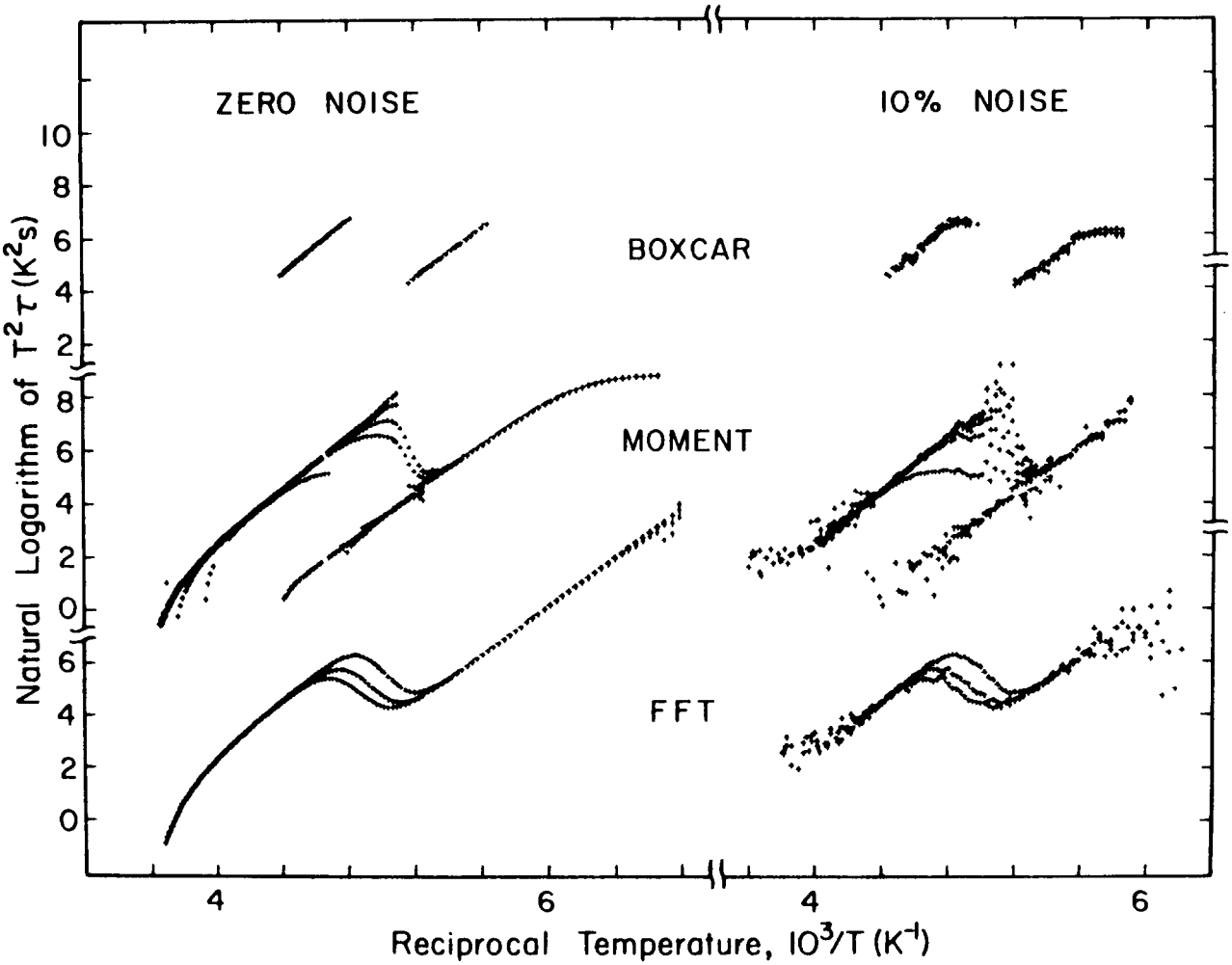

FIG. 4. Boxcar-, moment-, and FFT-derived activation energy plots for two equal-amplitude exponentials with 0 and 10% noise.

from the well-established formula[10,11]

$$1/\tau = \gamma\sigma T^2 e^{-\Delta E/K_B T},$$

where γ is presumed a constant for the material and carrier in question and K_B is Boltzmann's constant. The lowest noise results from the integer truncation error, which corresponds to about one sixty-four-thousandth of the peak-to-peak amplitude over the measured period. For higher noise levels, the program uses a pseudorandom number generator.

Rather than impose an arbitrary criterion for the closeness of fit, we will present the activation energy plots derived from the three methods. The natural logarithm of $T^2\tau$ is graphed versus $10^3/T$ for zero noise and a signal-to-noise ratio of 10. The slope of the line, therefore, is the activation energy ΔE divided by $10^3 K_B$. The relative merit of the various methods is reflected in the relative lengths over which the fits form a straight line, for it is this, combined with the absolute accuracy of each fit, that will allow for an accurate energy determination. The dispersion in the fits for a given temperature is due to different ratios of t_1 and t_2 for the boxcar, different depressions for moment, and different frequency terms for the FFT.

For single exponential components, the data were generated from published data for trap HB4.[10] Figure 3 presents the results. For 300 linearly spaced samples, the range of valid fits for the boxcar method is inherently restricted to just above two orders of magnitude. This degrades relatively rapidly with noise. The method of moments has a zero-noise range of over four orders of magnitude. Its degradation with noise arises from the difficulty in obtaining a reliable value for the baseline offset when confronted with noise. The FFT

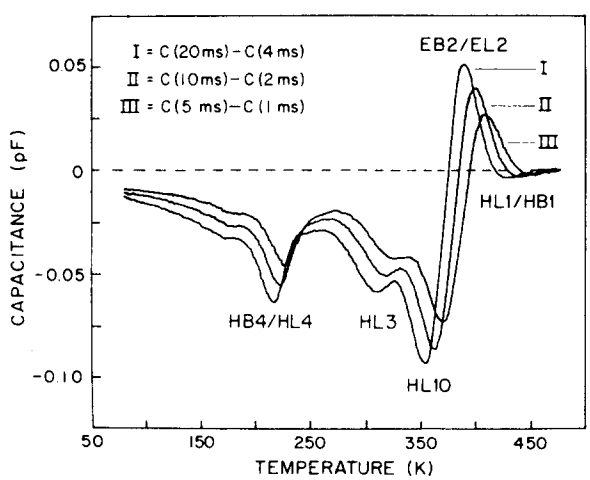

FIG. 5. Optical DLTS boxcar plots for a GaAs sample at different rate windows.

method, using 256 of the 300 samples, has a low-noise range exceeding even the method of moments. Increasing noise eventually predominates in the ratio of real to imaginary terms, causing the extracted α to be incorrect.

Figure 4 shows the results for two exponentials of equal amplitudes, derived from the activation energies and cross sections for the hole traps HB4 and HB5.[10] If the boxcar is allowed to start with the first sample, it yields a single activation energy somewhere between the two levels. Therefore, it must be started after, for instance, ten samples, with a corresponding decrease in the range over which τ can be extracted. In the presence of noise it quickly becomes incapable of providing ranges of valid fits that would allow accurate energy level assignment. The method of moments proves quite capable of extracting the two components, even in relatively severe noise. Importantly, the range over which one component can be extracted is not significantly affected by the presence of the other component. Without noise, the FFT does quite well. Its peformance in noise, however, is less remarkable.

It should be noted that when using single exponential analyses on multiple exponential data, it is impossible to decide which fits are valid, because there is no way in which to account for the other components when generating error statistics. Multiexponential analyses do not share this problem. The mean-square error for the method of moments will quickly identify the poor fits and enable them to be windowed out. But for the FFT and boxcar, there is no rational basis for selecting one fit over another.

A boxcar plot of optical DLTS data from a Schottky

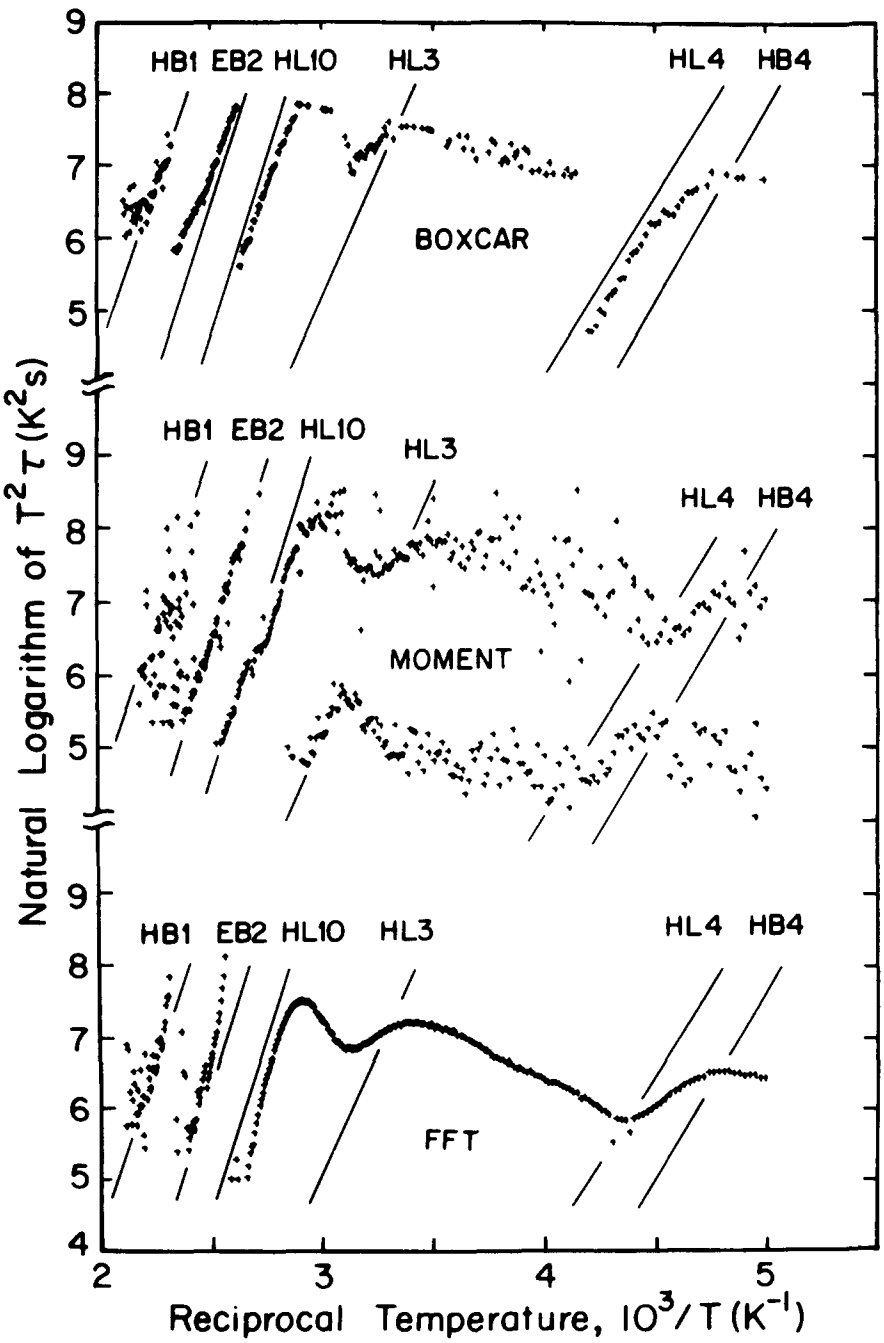

FIG. 6. Activation energy plots, via the three methods, for the experimental data of Fig. 5. The lines identify published activation energies and cross sections for traps in closest agreement to the experimental data. Decays outside the range of the fitting programs appear as more or less randomly distributed points, with a slight trend due to T^2.

TABLE I. The activation energies in eV and cross sections in cm^2 for the discernable traps in Fig. 5, as obtained by the three methods discussed in the text.

Trap energies and cross sections from different methods					
Method	Trap HB1/HL1	EB2/EL2	HL10	HL3	HB4/HL4
Refs.	0.78/0.94	0.83/0.825	0.83	0.59	0.44/0.42
10,11	$5\times10^{-16}/4\times10^{-14}$	$2\times10^{-13}/1\times10^{-13}$	2×10^{-13}	3×10^{-15}	$3\times10^{-14}/3\times10^{-15}$
boxcar	0.55 eV	0.74	0.71	0.25	0.39
	1×10^{-18} cm^2	1×10^{-14}	6×10^{-15}	4×10^{-21}	1×10^{-16}
moment	0.84	0.82	0.80	0.53	0.46
	4×10^{-15}	2×10^{-13}	8×10^{-14}	5×10^{-16}	4×10^{-14}
FFT	0.87	0.98	unstable	0.13	0.19
	5×10^{-15}	1×10^{-11}		8×10^{-23}	3×10^{-20}

diode on a vapor-phase epitaxial (vpe) layer of n-type GaAs is shown in Fig. 5. By comparing the peak locations and activation-energy spectra with published data, we identify the major peaks as levels HB4 (HL4) (copper), HL3 (iron), HL10[10] (vpe), and EB2 (EL2)[11] (vpe). In addition, HB1 (HL1)[10] (chromium) can be seen. The activation energy spectra of the levels are presented in Fig. 6. There are two important observations: First, it is generally accepted that the levels HB4 and HL4 are the same trap: splitting the difference is quite satisfactory. Second, the activation energy of the chromium center, HB1 (HL1), is not at all well determined, in part because the emission rate is highly dependent upon electric field.[2]

In order to present the data clearly, the graphs were produced by using the fit at each degree with the lowest mean-square error. Substantial care was exercised to ensure that this did not place either the boxcar of FFT methods at a disadvantage. In fact, it places the method of moments at a disadvantage by removing the weighting effect that several good fits at each temperature would give. From the comparison of the results for simulated and experimental data, it becomes apparent that the new analyses are at another disadvantage, because the capacitance meter is not quite fast enough and the ac coupled amplifier has a faster rolloff than previously believed. Both the method of moments and the FFT produce fits in the affected ranges, the boxcar does not. Without the new analyses, in fact, we would not even be aware of these problems.

The compression of the axes necessary to show the entire spectrum tends to make important differences seem trivial. This is shown in Table I, which presents the actual activation energies derived from the three methods. Due presumably to the presence of many levels, the boxcar and FFT methods often do not yield reasonably correct (or even plausible) activation energies and cross sections. The fundamental problem with these methods is that in the face of multiexponential behavior, error statistics are meaningless, and poor fits cannot be identified. Although matching the raw fits with published data can usually produce an identification of the trap (as done in Fig. 6), in some cases this identification would be incorrect. For instance, the boxcar's fits to the level we have identified as HL10 are closer to HL2, a level seen in liquid-phase epitaxial GaAs. The fact that the FFT is, in most cases, substantially worse than the boxcar indicates the severity of the nonexponential behavior. This was shown in Fig. 1, which plots the first 30 ms of the capacitance transient at 420 K, and appears to show at least three exponential components.

Despite the multiexponential behavior and the temporary limitations posed by the apparatus, the method of moments gives results that are closer to published results than the other methods. The ability to get definitive results becomes particularly relevant in the study of materials that have been less exhaustively characterized, for one may not have other's data to which to refer.

Undoubtedly, the published data were obtained by more or less conventional systems, but also from many measurement cycles over larger ranges of τ. Probably, the measurements were made on different samples better suited to the analysis of each trap, such as larger concentration for higher signal-to-noise and fewer competing traps at similar energies and concentrations. The method of moments gave us good results in considerably less time under less than ideal circumstances.

Having shown how the method of moments works, we are obligated to show where it encounters difficulties. Simultaneous positive and negative exponential decays occasionally confuse the baseline determination, producing unsatisfactory fits. Note that this did not prevent the analysis of the experimental data presented, but it did influence our choice of two exponentials of the same sign for the simulations. Large amounts of chromium in GaAs samples invariably causes the extracted activation energy for other traps to be lower than expected, due to the "cold emission" phenomenon.[2] We could circumvent this effect by otherwise ascertaining the emission rate of the chromium center at the temperature of interest (it is practically constant over hundreds of degrees) and forcing a solution for that number, much as we solve for the baseline. This would allow a more accurate determination of the residual, which contains the information about the trap of interest. Although inelegant solutions such as this may be necessary, we hope that these problems will be alleviated by general improvements in the method and its implementation.

COMPATIBILITY

There is no shortage of automated DLTS systems. Thus, the question of which systems are capable of imple-

menting these analysis techniques is highly relevant. In our opinion, some sort of graphics capability is a basic requirement. Manipulating the data without graphics is painstakingly slow and prone to error. Desk computer based systems without much memory or mass storage may not be able to accommodate the new methods, because the lack of mass storage necessitates that these analyses be performed during the experiment. This would be possible except that these calculators are rarely very fast, rarely support an assembly language or compiler-based language that could make them fast enough, and rarely have memory large enough to accommodate the combined measurement-analysis program.

Systems on computers larger than the LSI-11 are likely candidates for the implementation of advanced analyses. Their larger memories and higher computational speed will enable improvements in the methods outlined here, as well as the implementation of other methods. Many multiuser systems, however, are incapable of providing the control necessary for the experiment. Therefore, tandem systems are an optimum arrangement, where a dedicated computer runs the experiments and a large machine performs the analysis.

CONCLUSIONS

The method of moments is shown to be superior to conventionally used methods of analysis, for both simulated and experimental data. Further improvements may well be possible. The fast Fourier transform method is shown to be superior for the analysis of single exponentials, at little computational cost over the boxcar method.

Since the results derived from the method of moments usually correspond to other's observations, we can infer that the approximations made in determining capacitance from the trap population are usually acceptable. Barring blatant violations of those assumptions, the only major source of nonexponential behavior appears to be the presence of other deep levels.

ACKNOWLEDGMENTS

The authors thank C. E. C. Wood, D. W. Woodard, T. N. Jackson, J. D. Berry, M. Arkin, R. A. Stall, K. D. Fisch, J. V. Faricelli, and T. A. Benton for helpful discussions. Those from Cornell gratefully acknowledge support from IBM, General Electric, Rockwell International, and the Joint Services Electronics Program.

[1]E. E. Wagner and D. E. Mars, Rev. Sci. Instrum. **51**, 1205 (1980).
[2]S. Makram-Ebeid, G. M. Martin, and D. W. Woodard, "Phonon Assisted Tunnel Emission of Electrons from the *Cr* Level in GaAs," Int. Conf. on the Physics of Semiconductors, Kyoto, Japan (Sept. 1980).
[3]A. M. White, B. Day, and A. J. Grant, J. Phys. C **12**, 4833 (1979).
[4]C. R. Crowell and S. Alipanahi, Solid-State Electron. **24**, 25 (1981).
[5]I. Isenberg and R. Dyson, Biophys. J. **9**, 1337 (1969).
[6]I. Isenberg, R. Dyson, and R. Hanson, Biophys. J. **13**, 1090 (1973).
[7]R. Dyson and I. Isenberg, Biochemistry **10**, 3233 (1971).
[8]D. S. Day, M. Y. Tsai, B. G. Streetman, and D. V. Lang, J. Appl. Phys. **50**, 5093 (1979).
[9]A. Mitonneu, G. M. Martin, and A. Mircea, Inst. Phys. Conf. Ser. 33a, Chap. 2 (1977).
[10]A. Mitonneu, G. M. Martin, and A. Mircea, Electron. Lett. **13**, 666 (1977).
[11]A. Mitonneu, G. M. Martin, and A. Mircea, Electron. Lett. **13**, 191 (1977).